Excess Loss Model for Low Elevation Links in Urban Areas for UAVs

Michal SIMUNEK[1], *Pavel PECHAC*[1], *Fernando P. FONTAN*[2]

[1]Dept. of Electromagnetic Field, Czech Technical University in Prague, Technická 2, 160 00 Praha 6, Czech Rep.
[2]Telecommunications Engineering School. University of Vigo, Campus universitario, 36310 Vigo, Spain.

simunmi1@fel.cvut.cz, pechac@fel.cvut.cz, fpfontan@tsc.uvigo.es

Abstract. *In this paper we analyze the link between an UAV and a ground control station in an urban area. This link shows a unique geometry which is somewhere in between the purely terrestrial (e.g., a macro-cell channel) and the land mobile satellite case (LMS). We describe a measurement campaign which reproduces the UAV link conditions and shows how the excess loss is mainly dependent on the elevation angle and fairly independent of the distance. Finally, we propose a simple physical model for predicting the excess loss based on a combination of diffracted and reflected components. Results from this model are in good agreement with the measurements.*

Keywords

UAV, channel modeling, low elevation, urban area, path loss, diffraction.

1. Introduction

Nowadays, civilian applications including air surveillance, remote sensing, law enforcement, etc. can be implemented by means of remotely controlled, **u**nmanned **a**erial **v**ehicles. These aircraft are commonly called UAVs. They are usually controlled and operated from distant locations using low frequencies (VHF, UHF) guarantying a sufficient maximal range and supporting low data rates for telecontrol and telemetry. However, for high data rates, another, higher frequency link is required. This link is used to send back to base the images (SAR, radiometer, ...), sensor data, or any other information gathered during normal operation, as onboard storage would increase the payload weight and because real-time data processing may be needed, not feasible onboard. The frequencies of interest are in the UHF range where diffraction, reflection and multipath effects dominate. Representative measurements have been performed at 2 GHz.

The geometry of this high data rate link is shown in Fig. 1. The elevation angle may usually go from about 1° to 5°. Links with this type of geometry can be classified as "Low Elevation Links".

For planning and deploying such systems, a good understanding of the signal propagation phenomena involved is required. Propagation is a complex random process encompassing many possible contributions. Normally, as most other channels, its narrowband behavior can be broken down into three rates of change: fast, slow and very slow variations. We will be concentrating here on the very slow variations usually characterized by means of the *excess loss*.

A full statistical study of the slow and fast variations, mainly due to multipath, is out of the scope of this paper and will be presented in detail at a later time.

For developing a model capable of providing information on the path loss for a specified geometry, there is a need of understanding the principles which have influence on final received signal. In this paper we will study the diffraction and reflection phenomena for this specific geometry and based on this information we will develop a new simple physical model.

This model should provide guidance on the kind of attenuation levels to be expected when the control station in urban areas is at street level; this can be considered as a worst case scenario where the control station is totally surrounded by buildings and no alignment of the street with the link exist (waveguide effect) Alternative settings for the controlling station above the nearby rooftops may not be possible in some operational cases.

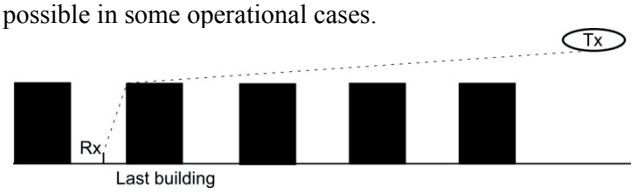

Fig. 1. Geometry of a link between UAV and a ground control station.

Many models for narrowband terrestrial services and for land mobile satellite services (LMS) are available, but low elevation links require further study. Here, we will be trying to extend the work performed in the frame of terrestrial services for assessing the observed path loss. The geometry of this link is similar, albeit with elevation angles slightly higher, to those of macro-cell links where the base station antenna is located above the buildings in its vicinity.

Several prediction methods are available which could be adapted to model the path loss for this low elevation link. Several methods to model macro-cell links are reviewed in [1]: empirical models such as the Hata-COST 231 model, Okumura-Hata, Lee, or physical models such as the Walfish-Ikegami COST 231, Walfish-Bertoni or the Flat Edge Model.

We have arrived at the conclusion that, unlike in the terrestrial case, where the multiple diffraction effects on the rooftops of several consecutive buildings must be taken into consideration due to the grazing angles involved, in this case, the last building in the path, i.e., the one closest to the receiver terminal in the direction of the UAV, is the only diffracting element to be taken into consideration. This last building can be very well approximated by two adjacent knife edges. Additionally, it is important to include the effect of the ray reflected on the opposite side of the street. The power sum of these two rays provides an excellent approximation for estimating the excess loss. Moreover, for the diffraction study, we put this model in the context of other well-known models [1], mainly for terrestrial links, where more than two rays, up to four, are identified to have a significant influence on the excess loss. These additional rays will, in our case, have an impact on the slow and fast variations undergone by the signal.

We have performed a unique measurement campaign at 2 GHz simulating an UAV by means of a remotely controlled airship. In this paper we focus on the path loss dependence on the link geometry and suggest an accurate but simple method to model the excess loss in urban areas. The *excess loss* is defined as the difference between the actual path loss and the free space loss.

This paper tries to contribute new experimental results and an excess loss model in this relatively new field where only a limited number of publications, e.g. [2] [3] [4], are available.

2. Experiment Trials

In this section we discuss the experiment carried out, review the data processing performed and briefly comment on the type of results obtained.

2.1 Measurement Setup

To study the UAV channel in urban areas we have chosen a fairly flat and uniformly built-up district of the city of Prague, Dejvice, whose area is approximately 570×580 m^2, where the buildings are of a similar type, made of brick, of about 22 m in height, built in 1922. Street widths are in the order of 17 m (Fig. 2).

A remotely controlled airship [5] was used to simulate an UAV. The airship flew from and toward the receiver at approximately constant azimuths from a distance of 1.2 to 6.5 km in flight levels from 150 m to 300 m above ground. Thus, from the ground control station the UAV was seen under elevation angles from 1.6° to 6.5°. In the study presented in this paper, only the azimuths perpendicular to the street direction were kept for the analysis.

A continuous wave (CW) transmitter with a carrier frequency of 2 GHz connected to a monopole antenna was placed on the bottom side of the remotely controlled airship. During the flights, GPS position data were stored. To increase positioning accuracy, differential post-processing was performed. The airship system also provided the capability to store pitch and roll data which were used to discard invalid sections of the data with high pitch/roll angles, as possible large polarization or antenna pattern losses could have taken place, as well as partial shadowing of the transmit antenna.

A four-channel receiver for performing diversity studies was set up (Fig. 4). As shown, four quarter-wave monopoles with rod ground planes were used. The same antenna type was used at the transmit side. The receiver was developed at the Dept. of Electromagnetic Fields, Czech Technical University. It allows simultaneous measurements at four channels. The sensitivity was −126 dBm for a measurement bandwidth of 12.5 kHz. The transmitted power was 27 dBm, the signal being an unmodulated carrier (CW).

The recording rate was 100 samples per second. The receiver was connected to the four monopoles forming a square of side 22.5 cm (1.5 λ). The antennas were placed 1.5 m above street level (Fig. 4). In this paper, data from a single antenna is analyzed while further studies including statistical modeling and diversity analysis will be presented at a later time. However, consistency checks between the path loss values measured in all four channels were carried out to verify the quality of the measurements.

The receiver was placed at two different, representative locations simulating possible positions of the UAV receive station (Fig. 2 and Fig. 3). The first position – location #1 – was chosen by trying to get as far as possible from the nearest building in the direction of the UAV, thus minimizing the diffraction loss. The second position – location #2 – corresponds to the worst case scenario where the receiver is very close to the building in the direction of the UAV (Fig. 2 and Fig. 3). The reader is reminded that the airship flight paths were perpendicular to the street.

2.2 Data Processing

During the measurements, received power data plus auxiliary information were recorded to different devices: position data was stored in a GPS device, flight data including pitch and roll were stored to the operator notebook through the UAV control communication link and, finally, the received data was stored to a notebook attached to the test receiver. All data sources were time stamped for off-line synchronization at the post-processing stage. The clocks of the notebooks were synchronized to the GPS time prior to performing the measurements.

Fig. 2. Receiver locations #1 and #2 (image from Google Earth), in Dejvice, city of Prague.

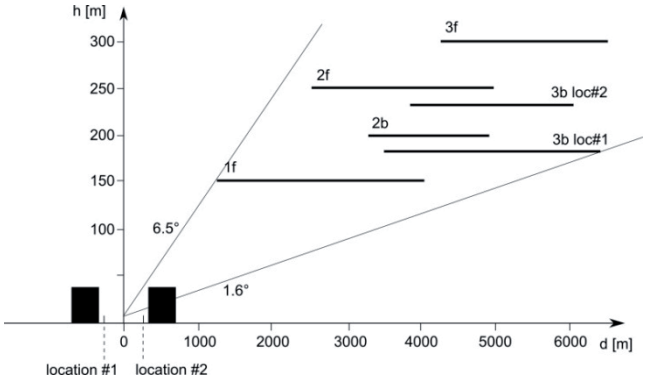

Fig. 3. Flights and receive antenna locations used in this study.

Fig. 4. Receive antenna diversity arrangement at street level.

Once all data sources were synchronized, invalid data due to large pitch or roll values were flagged out. The acceptable limits for both angles were set to a maximum of 10°. The fast, multipath-induced variations were removed by low pass filtering. The averaged signal series was used for comparison with model predicted levels as discussed later on. Several window sizes were tested; finally a size of 4,000 wavelengths (600 m) was found to adequately remove the slow and fast variations, leaving in only the very slow variations. Averaging was performed on linear power levels which were then converted to logarithmic units.

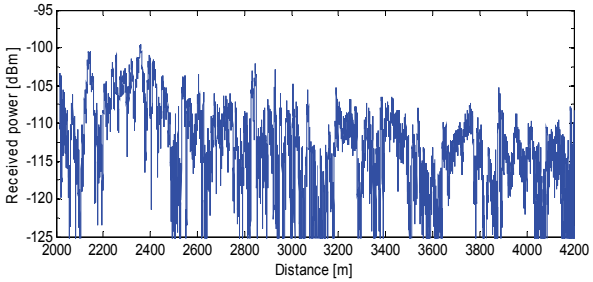

Fig. 5. Example of path loss series as a function of distance for test flight 1f, Rx location #2 (Fig 3).

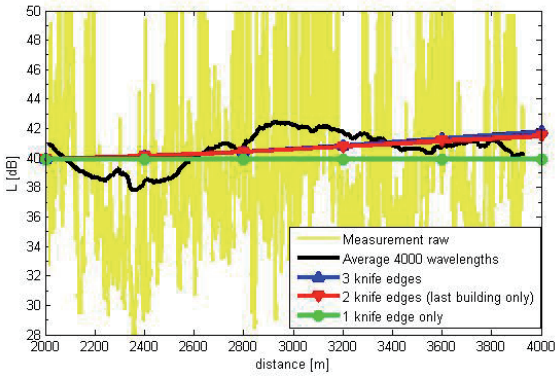

Fig. 6. Model and measured data (row excess loss and filtered). Location #2, flight 1f.

Finally, the total path loss was calculated from which the free space loss (FSL) was subtracted to calculate the excess loss, L (dB). Fig. 5 illustrates a path loss series as a function of the distance from the receiver for test flight 1f, Rx location #2 (Fig. 3).

2.3 Results

The excess loss, L (dB), calculated from the measured data was plotted as a function of the distance to the airship. Very strong variations due to specular reflections, especially between 2 and 2.2 km (Fig. 5 and Fig. 6), and to diffuse multipath throughout, were observed in the measured series. To facilitate the comparison between predicted and measured excess losses, a running mean filter was used to remove the slow and fast variations. Fig. 6 illustrates the measured excess losses after low-pass filtering for the path loss series in Fig. 5. This figure also shows modeling results which will be discussed later on.

In Fig. 6, the data taken at Location #2 (Rx on the Tx side of the road, closest to the blocking building) is shown. The general behavior is that, once the free space component, which depends logarithmically on the distance as 20 log(d), has been removed, we can observe a fairly distance-independent trend. It is rather the elevation that significantly determines the excess loss. Standard terrestrial empirical models like Hata-COST 231 [6] are strongly dependent on the distance; this makes this type of models not particularly suitable for use in low elevation links such

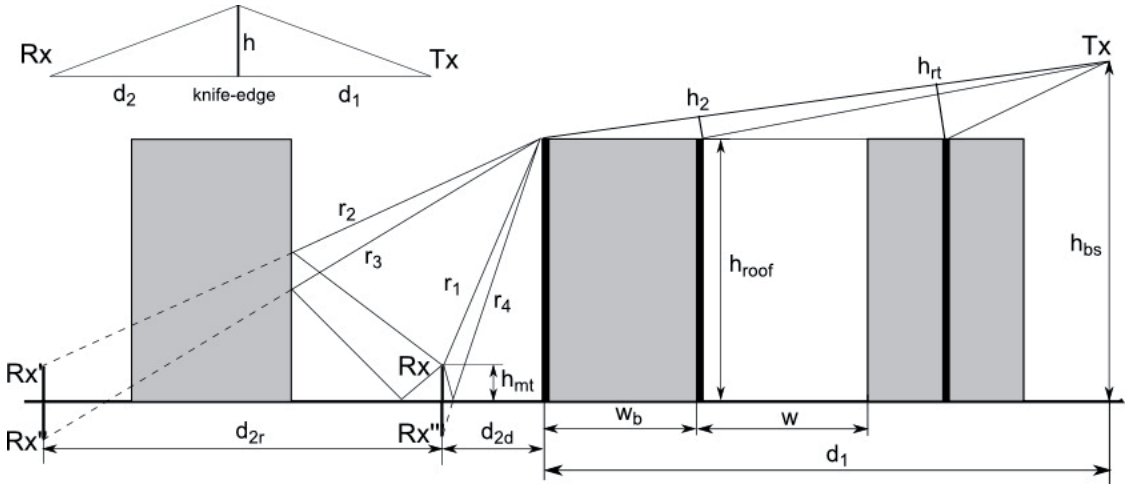

Fig. 7. Overall propagation scenario and possible diffracted and reflected paths.

as those found in UAV applications. The data taken at location #1 (Rx on the Tx opposite side of the road) also confirmed the above observations.

3. Excess Loss Modeling

3.1 Basic Approach

To find a suitable method to model the excess loss, we considered the physical mechanisms involved. The main factor influencing the excess loss is diffraction. Following the well-known Walfisch-Ikegami (COST 231) model, the propagation path between transmitter and receiver can be broken down into two parts, each being affected by different diffraction mechanisms. Also in the proposed model, initially, the total contribution will be divided up into two components: the diffraction loss due to the last building, L_{lb}, and the diffraction loss due to the various buildings between transmitter and the last building, L_{rt} (roof tops), which are included in the first Fresnel zone. Each of these two components should be computed separately, the total excess loss being their sum, i.e.,

$$L_{\mathrm{t}}(\mathrm{dB}) = L_{\mathrm{lb}} + L_{\mathrm{rt}} . \tag{1}$$

This approach is used in many semi-deterministic models like the Flat Edge Model by Saunders [7], the Walfisch-Bertoni model [8], or the already mentioned Walfisch-Ikegami (COST 231) model [6].

3.2 Path Loss Due To the Last Building

There are several methods which can be used to model the diffraction due to a building. In our case, the buildings of interest are old brick apartment buildings of about 22 meters in height with gable (triangular) roofs. These buildings are very complex in shape with many non-uniformities such as windows, roof windows, chimneys, etc. Their effects will be considered statistically as pertaining to the slow variations superposed on slower ones included in the excess loss. One of our initial objectives was developing a physical model with an easy to use formulation. Thus, we have described each of the intervening buildings by means of one or two knife-edges. This approach has been shown to produce fairly accurate results [1] in terrestrial path geometries.

UAV links are unique in the short distances from the receiver to the obstructing edge. Most previous works assume that the distance between receiver and obstruction, and between transmitter and obstruction (d_1, d_2, Fig. 7) are much larger than the obstruction height (h). In this case, d_1 is much larger than h but d_2 is usually of similar or smaller magnitude than h. Hence, we cannot model the last building by means of a single knife-edge obstruction located in its center. A solution which takes into account the short distances from receiver to obstruction is proposed in Rec. ITU-R 526 [9], which suggests modeling the building by means of two knife edges on both outer walls, Fig. 7.

The excess attenuation due to the nearest building can be calculated using an approximate multiple knife-edge diffraction approach, Deygout's method being optimum for the case where one edge dominates over the other [10]. This approximation identifies a main diffracting edge, the one closest to the receiver in this case, giving rise to a loss L_{lb1}. To this we need to add the attenuation due to the secondary knife-edge, L_{lb2}, which affects the line of sight between the top of the first knife-edge and the transmitter. The overall excess loss is thus given by

$$L_{\mathrm{lb}}(\mathrm{dB}) = L_{\mathrm{lb1}} + L_{\mathrm{lb2}} . \tag{2}$$

We have so far only analyzed one of the possible paths, however, the received signal at street level may be composed of many rays; of those, the most significant ones (Fig. 7) are [11] the direct ray (1) reaching the receiver after being diffracted on the building on the transmitter side, and two possible specular reflected rays, one on the building on the opposite side of the street (2) and other on

the ground (4). These two contributions also undergo diffraction before being reflected. Other possible reflected contribution would be one suffering a double reflection on the building opposite and on the ground (3). In addition, there is diffuse multipath as shown in Fig. 5. Diffuse multipath will be considered in the fast variations part of the model, out of the scope of this paper. As in [11], [12], for assessing the excess loss we can consider the power sum of the direct and one or more of the three reflected rays just discussed, Fig. 7. The general formula for the average received field, E, i.e., taking into account all possible reflections, can be expressed as a root mean square of the field strengths of components taken into consideration, as proposed Ikegami [12], i.e.,

$$E\,(\mathrm{dBV/m}) = 10\log\left(\sum_{n=1}^{4} {e_n}^2\right). \tag{3}$$

The intensities in linear units are represented by lower-case letters while, when in logarithmic units, we use capital letters. In this paper we will be using the excess loss, L (dB), instead of field strength, E, i.e.,

$$L\,(\mathrm{dB}) = -10\log\left(\sum_{n=1}^{4} \frac{1}{10^{L_n/20}}\right). \tag{4}$$

Thus, the general expression for the excess loss resulting from the combination of the four rays considered, all undergoing diffraction on the closest knife-edge on the transmitter side of the street is given by

$$L\,(\mathrm{dB}) = -10\log\left(\frac{1}{10^{L_1/20}} + \frac{r_\mathrm{b}^2}{10^{L_2/20}} + \frac{r_\mathrm{b}^2\, r_\mathrm{g}^2}{10^{L_3/20}} + \frac{r_\mathrm{g}^2}{10^{L_4/20}}\right) \tag{5}$$

where L_1 to L_4 (dB) are the diffraction attenuations affecting the individual rays, r_b (linear) is the magnitude of the building reflection coefficient and r_g is the magnitude of the ground reflection coefficient.

The excess loss caused by diffraction can be computed using the Fresnel integrals [13]. For this geometry where the building height, h_roof, is larger than the street width, w, the normalized obstruction parameter, v, is greater than 10; in this case we can use the following approximation of the Fresnel integrals,

$$\frac{e}{e_0} = \frac{0.225}{v} \tag{6}$$

where e is the actual received field and e_0 is the free space under line of sight conditions. The above expression in terms of the excess loss and in dB, is given by

$$L\,(\mathrm{dB}) = -20\log\left(\frac{0.225}{v}\right) \tag{7}$$

which shows a perfect agreement for $v > 2.5$. In general, the parameter v is defined as [9]

$$\nu = h\sqrt{\frac{2}{\lambda}\left(\frac{1}{d_1} + \frac{1}{d_2}\right)} \approx h\sqrt{\frac{2}{\lambda d_2}} \tag{8}$$

where its elements are graphically depicted in Fig. 7. The approximation is valid when $d_2 >> d_1$.

As an approximation, out of the three reflected rays, we will be only considering the wall reflected ray, i.e., ray-2. We are trying to reproduce the level and evolution of the very slow variations, i.e., smaller scale features has been removed. Unless the disagreement between measurements and model is unacceptable, we will not introduce further rays, thus keeping the model simple. In [12] only two rays, the direct and the reflected, were considered.

For the main diffracting edge, $h \approx h_\mathrm{roof} - h_\mathrm{mt}$ and $d_2 \approx d_\mathrm{2d} \approx d_\mathrm{w}$, for direct ray and $d_2 \approx d_\mathrm{2r} \approx (2w - d_\mathrm{w})$, for reflected ray (Fig. 7). Therefore, using (7) and (8) we get a final form of last building main knife-edge attenuation L_lb1,

$$L_\mathrm{lb1} = -10\,\log\left[\frac{0.05\,\lambda}{2(h_\mathrm{roof} - h_\mathrm{mt})^2}(d_\mathrm{w} + R_\mathrm{b}^2(2w - d_\mathrm{w}))\right]. \tag{9}$$

The parameters for calculating the diffraction loss due to the second edge (secondary edge) can be computed following Deygout's method (Fig. 7). In this case, the excess height parameter, ν, for the second edge will be negative. Here, we will use a simple exponential approximation of the Fresnel Integral which ignores the oscillations in the field strength for $v < -1$, i.e.,

$$L_\mathrm{lb2}\,(\mathrm{dB}) = -20\log(1 - e^k) \tag{10}$$

which shows sufficient agreement for $v < 0$, and where

$$k = -0.6038 \cdot 0.1094^{v} \tag{11}$$

with v as defined in (8). The inverse of distance d_1, $1/d_1$, can be neglected; d_2 is represented by w_b, and h_2 (Fig. 7) is given by

$$h_2 \approx -w_\mathrm{b}\sin\left(\tan^{-1}\left(\frac{h_\mathrm{bs} - h_\mathrm{roof}}{d - d_\mathrm{w}}\right)\right). \tag{12}$$

The diffraction parameters for ray 2 (and rays 3 and 4 if necessary) can be calculated in a similar way by considering the appropriate images of the receiver with respect to either of both the wall on the opposite side of the street or the ground.

3.3 Diffraction at Multiple Rooftops

For this scenario, given the low elevation angles involved, it might be necessary to take into account the additional diffraction loss introduced by the multiple buildings in between the transmitter and the building nearest the receiver. This term is often found in propagation models such as the Walfisch-Ikegami (COST 231) model [6].

Given the geometry depicted in Fig. 7, where the elevation angle from the top of the last building may go from 1.4 to 5.6 degrees at most, it will be necessary to consider only one additional rooftop in the direction of the

transmitter. All additional edges will introduce a negligible increase in the attenuation. Due to the large distances from the obstacle, we can use a standard representation of the building by means of a knife-edge in the middle of the building. In this case, the excess height, h_{rt}, will also show negative values. Thus, we will use the same method as in the second knife-edge belonging to the last building, i.e.,

$$L_{rt}(\text{dB}) = -20\log(1-e^{k}) \tag{13}$$

where k is defined in (11) and v in (8) (Fig. 7), h is given by

$$h_{rt} \approx -(1.5w_b + w)\sin\left(\tan^{-1}\left(\frac{h_{bs}-h_{roof}}{d-d_w}\right)\right). \tag{14}$$

The inverse distance, $1/d_1$, can be neglected and d_2 is equal to $1.5w_b+w$.

As said, the complete approach has been described above for completeness; however, some of the above terms will be negligible and will be disregarded in the final model after its verification and validation.

4. Model Verification and Validation

4.1 Model Verification

Before going on to compare the measured data and model predictions, we have verified the heuristic approximations for diffraction included in the proposed model, i.e., Deygout's approach. Thus, we have followed the guidelines in [14] where the Fresnel-Kirchhoff (F-K) theory is applied to vertical 2D profiles using a paraxial approximation and performing a discrete integration over each successive screen (knife-edge). We have modified the Matlab codes provided in [15] adapting them to the UAV link geometry. Fig. 8 sketches the simulated scenario. We kept the receive antenna at a constant height of 1.5 m while we simulated an UAV flight at a constant height of 150 m for a distance range from 1.2 to 4 km.

Fig. 9 shows a comparison between the predictions with the proposed model and those obtained using F-K for the direct ray only. We can observe how the agreement between the F-K simulations for two edges is within one dB of our model's prediction assuming 2 edges. In the figure we also show how introducing one third edge does not change the prediction. In the F-K calculations, introducing one or two further edges changes only slightly the loss. Thus, we can conclude that, for the geometry under consideration, two edges should provide a reasonably good prediction.

We can also notice the difference between the F-K simulation and our model for only one knife-edge, where their values should follow the same trend. This difference is due to the simplification in the expression for the v parameter, Eq. 7, for the first diffracting edge. We do not consider the theoretical gain of the knife edge diffraction

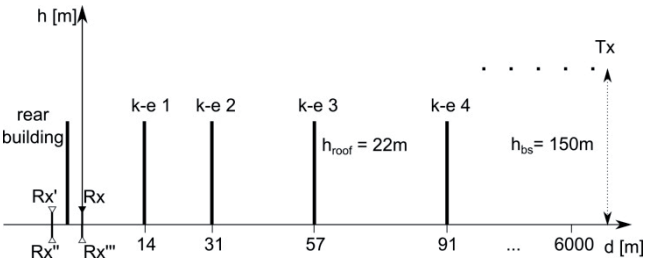

Fig. 8. Simulated scenario using our model and F-K.

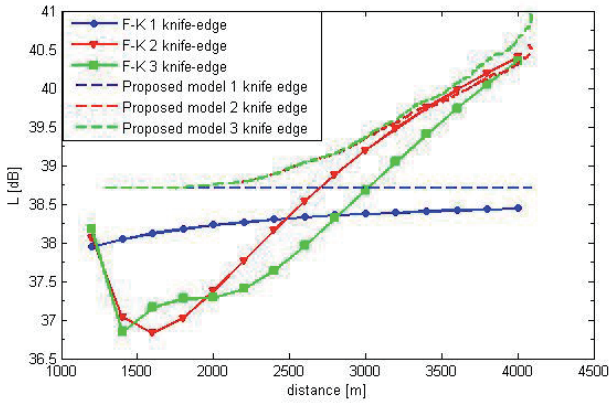

Fig. 9. Evaluation of importance of including more diffracting edges for assessing the direct signal level in our model and for F-K.

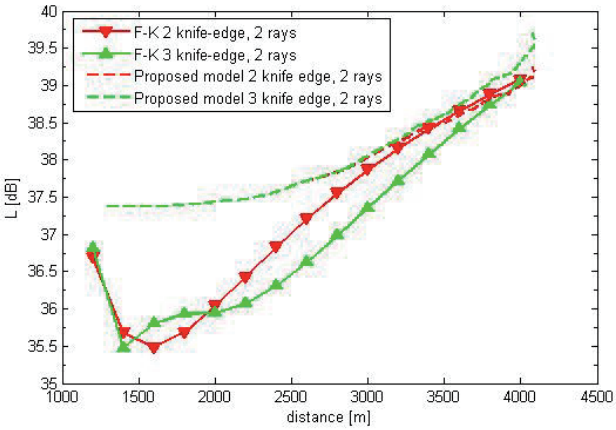

Fig. 10. Comparison between our model and F-K for two and three diffracting edges, assuming two rays: direct and reflected.

for $v < 0$ [1]. As said before, this is for keeping the model as simple as possible.

Now, in Fig. 10, we go on to analyze the model assuming two rays, the direct and a reflected ray on the building on the opposite side of the street. We have only considered two and three diffracting edges in this case. In the figure we can see how our model and the F-K calculations tend to produce similar results for the longer distances simulated. For the shorter distances, the error is not larger than 1.5 dB, which we consider to be acceptable, since we are attempting to develop a simple mode valid for the whole distance range, with special emphasis on the longer distances (>3 km). We will come back to this issue in the following section.

4.2 Model Validation

To verify the model, we compared the excess loss from the low-pass filtered measured data with predictions using the proposed model using only rays 1 and 2. Already in Fig. 6 we showed measured excess losses for test flight 1f, Rx location #2 (closest to the nearest building). Also in the figure predictions made assuming one, two or three diffracting edges are shown. We can observe a very good agreement between the measurements and the predictions in all three diffraction configurations. However, it is clear that introducing a third diffracting edge does not improve the prediction.

In the same way, in Fig. 11 we show the same flight path for Location #1 (furthest from the nearest building in the direction of the transmitter). Observing both Fig. 6 and Fig. 8, we can notice a significant gain of about 5 dB when we move away from the first building.

As for the differences between predictions and measurements in Fig. 11, we can observe an excellent match for distances in excess of 2.5 km, i.e., for the lowest elevations in the considered range. Differences not exceeding about 5 dB can be observed for the shorter distances, i.e., for the highest elevations in the range under study. We predict higher losses than the actual ones. These differences could be compensated for by including rays 3 and 4. However, we are looking for a simple model which provides good predictions throughout the elevation angle/distance range of interest, and the accuracy achieved is reasonable enough. This can also be confirmed by the results in Tab. 1, as discussed next.

It must also be pointed out that the overall envisaged model will also include slow and fast variations. With reference to the slow variations observed both in Fig. 6 and Fig. 8, the prediction errors will be somehow mixed with or included in the long-term variability about the mean of the excess loss, i.e., the standard deviation of the error in Tab. 1.

It has been found that the contribution of the third knife-edge (that represents buildings other that the last one) is negligible, in the order of a faction of a dB, while introducing the second knife-edge improves the agreement between the model and the measurements. The building reflection coefficient, r_b, was set to 0.5, i.e., –6 dB, as in [12]. In other works, e.g. in [11], a value of 0.3 (–10.45 dB) is used.

The model was derived for distances ranging from approximately 1.2 to 6 km and transmitter heights, h_{bs}, from 150 to 300 m, however, due to the elevation angle dependence in the model, it should be valid for greater distances giving rise to elevations in the same range, i.e., from approximately 1.5 to 6 deg.

Two error parameters were computed: the mean error (ME) and its standard deviation (STD) expressed in dB. The error is defined as the difference between the measured excess loss after (4000 wavelength) averaging and the predicted values using two rays. The comparisons of individual flights, measurement locations and overall results are summarized in Tab. 1.

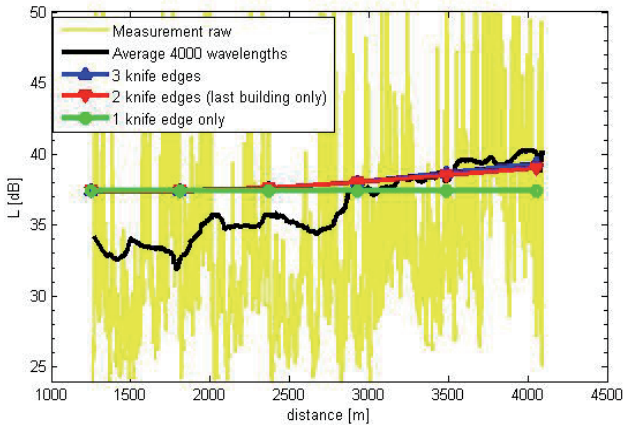

Fig. 11. Model and measured data (row excess loss and filtered). Location #1, flight 1f.

Location #1	ME [dB]	STD [dB]	Path length (m)
1f	-1.67	2.51	2810
2f	-0.42	1.35	2285
2b	1.54	2.42	1490
3f	-0.42	0.85	2154
3b	1.19	1.62	2800
Overall #1	0.14	2.71	
Location #2	ME [dB]	STD [dB]	Path length (m)
1f	-0.11	0.97	2158
2f	-0.01	0.79	1719
2b	1.29	2.28	877
3f	0.09	1.26	2046
3b	0.22	1.30	2328
Overall #2	0.29	1.7	
Overall #1 & #2	0.06	2.2	

Tab. 1. Comparison results with objective parameters.

The values in the table show a good general agreement between the measured data and model. There are deviations caused by the slow and very slow variations which cannot be predicted with this model, but the model follows quite well the observed trend in its entirety. As in Fig. 11, the errors become larger for the highest elevations contained in the various flight paths. However, the overall error statistics are quite good, which leads us to stay with the simplest model configuration, i.e., two diffracting edges and two rays: direct and wall reflected.

5. Conclusions

In this paper we have presented results from a measurement campaign simulating the conditions typical in UAV high data rate communication links in urban areas at frequencies of about 2 GHz. We have observed strong signal variations due to multipath and shadowing suggesting an overall model resulting from the combination of

two distributions, one for the slow and the other for the fast variations. We have concentrated here on assessing the average signal loss expressed as the excess loss with respect to free space, and its variations with distance and elevation. Also two possible control station locations at street level within the urban area have been considered, one close to the nearest building in the direction of the UAV and the other on the opposite side of the street.

A model for the excess loss has been developed. It is based on existing models for terrestrial macro-cells, although the elevation angles involved are larger in this case. The proposed model is a combination of diffraction on the nearest building and reflection off the building opposite. Building diffraction has been modeled by assuming two knife-edges set on both external walls of the building under consideration. Unlike in terrestrial links where grazing incidences are usual, no further buildings need to be taken into account.

Acknowledgements

This work was partly supported by the Czech Ministry of Education, Youth and Sports under research project no. OC09074 in the frame of COST Action IC0802.

References

[1] SAUNDERS, S., ZAVALA, A. *Antennas and propagation for wireless communication systems*. 2nd ed.. New York: Wiley, 2007.

[2] ROMEU, J., AGUASCA, A., ALONSO, J., BLANCH, S., MARTINS, R. Small UAV radiocommunication channel characterization. In *Fourth European Conference on Antennas and Propagation (EuCAP)*. Barcelona (Spain), 2010, p. 1 - 5.

[3] CERASOLI, C. An analysis of unmanned airborne vehicle relay coverage in urban environments. In *Military Communications Conference (MILCOM)*. Orlando (USA), 2007, p. 1 - 7.

[4] IGLESIAS, D., SANCHEZ, M., ALEJOS, A., CUIÑAS, I. Empirical propagation model for low elevation satellites. In *IEEE Wireless Technology Conference (EuWIT)*. Paris (France), 2010, p. 13 - 16.

[5] *AirshipClub* [Online]. Available at: http://www.airshipclub.com.

[6] CICHON, D. J., KÜRNER, T. *Propagation Prediction Models*. COST 231 Final Report, Chapter 4, 1999.

[7] SAUNDERS, S., BONAR, F. Explicit multiple building diffraction attenuation function for mobile radio wave propagation. *Electronics Letters*, 1991, vol. 27, no. 14, p. 1276 - 1277.

[8] WALFISCH, J., BERTONI, H. A theoretical model of UHF propagation in urban environments. *IEEE Transactions on Antennas and Propagation*, 1988, vol. 36, no. 12, p. 1788 - 1796.

[9] ITU-R Rec. P.526-11, *Propagation by Diffraction*. ITU, 2009.

[10] PARSONS, J. *Mobile Radio Propagation Channel*. 2nd ed. New York: Wiley, 2000.

[11] BERTONI, H. *Radio Propagation for Modern Wireless Systems*. Upper Saddle River (USA): Prentice Hall, 2000.

[12] IKEGAMI, F., YOSHIDA, S., TAKEUCHI, T., UMEHIRA, M. Propagation factors controlling mean field strength on urban streets. *IEEE Transactions on Antennas and Propagation*, 1984, vol. 32, no. 8, p. 822 - 829.

[13] BARCLEY, L. *Propagation of Radiowaves*, 2nd ed. IEE, 2003.

[14] WHITTEKER, J. H. Fresnel–Kirchhoff theory applied to terrain diffraction problems. *Radio Science*, 1990, vol. 25, no. 5, p. 837 - 851.

[15] PEREZ FONTAN, F., MARIÑO ESPIÑEIRA, P. *Modelling the Wireless Propagation Channel. A Simulation Approach with Matlab*. New York: Wiley, 2008.

About Authors ...

Michal SIMUNEK was born in Prague. He received his M.Sc. from Czech Technical University in Prague in 2009. Currently he is working towards his Ph.D. at the same university, where his researching interests include propagation channel modeling for UAVs. During this period he has actively collaborated in ESA PECS project no. 98069, Building Penetration Measurement and Modeling for Satellite Communications at L, S and C-Band 2009-2010 and COST IC0802 Propagation tools and data for integrated Telecommunication, Navigation and Earth Observation systems.

Pavel PECHAC received the M.Sc. degree and the Ph.D. degree in radio electronics from the Czech Technical University in Prague, Czech Republic, in 1993 and 1999 respectively. He is currently a Professor in the Department of Electromagnetic Field at the Czech Technical University in Prague. His research interests are in the field of radiowave propagation and wireless systems. More details can be found at http://pechac.elmag.org.

Fernando PÉREZ FONTÁN Born in Villagarcía de Arosa, Spain. He obtained his degree in Telecommunications Engineering in 1982 from the Technical University of Madrid and his PhD in 1992 from the same university. After working in industry since 1984 he became an assistant professor at the University of Vigo in 1988. In 1993 he became an associate professor and in 1999 a full professor with the Signal Theory and Communications Department of the University of Vigo. He lectures in Radiocommunication Systems, especially in terrestrial fixed and mobile system related topics. He is the author of a number of books and journal papers and has been the leader in several projects funded by public and private entities. He participates in ITU-R WG3 on Propagation Modeling. He has been Management Committee Member of EU' COST 255, 280 and 297, and currently participates with the same role in COST IC0802.